

Radar Cross-section Reduction of Planar Absorbers Using Resistive FSS Unit Cells

Mustafa B. Jasim and Khalil H. Sayidmarie

Ninevah University, Mosul, Iraq

<https://doi.org/10.26636/jtit.2023.4.1331>

Abstract — This paper demonstrates the feasibility of reducing radar cross-section by employing resistive sheets or rings in the conducting elements of an FSS unit cell. The idea behind the approach in question is to create power-absorbing elements which may help reduce the power reflected from FSS surface. The investigated FSS unit cells have the form of double-closed rings and double-closed-split rings. A carbon paste, serving as the resistive layer, was inserted in various regions within the unit cell. The CST Microwave Studio software was used to obtain the reflection coefficient. Specific dimensions and conductivity of the paste were selected to ensure better performance. Simulation results showed that the reflection coefficient may be reduced by 8 dB, to 14 dB, by using carbon paste with the conventional copper layer.

Keywords — carbon paste, double rings, FSS, radar cross-section reduction, resistor, unit cell

1. Introduction

Radar stealth technology has advanced rapidly over the past few years, leading to novel techniques for lowering radar cross-section (RCS) values. Various approaches to RCS reduction, including shape tailoring and material absorption, have been proposed in the past decade. In the case of frequency-selective surfaces, the absorption method is used, in which the Dallenbach layer and other resonance absorbers are positioned on a conducting plane to convert the incident electromagnetic energy to heat [1]. Salisbury screens were also employed as absorbers, using a resistive sheet placed over a metallic surface at a distance of 1.25 wavelengths. However, significant thickness and limited bandwidth of those layers prevent them from being used on moving platforms [2].

An RCS reduction of 10 dB is typically considered sufficient for practical purposes [1]. The radar cross-section is reduced by 90% when a 10 dB mitigation is obtained for any target. The two main processes used to reduce the RCS of an object were absorption and scattering. In the case of the absorption approach, all or significant portions of the incident wave's power are absorbed by a frequency selective surface (FSS) layer. Meanwhile, scattering refers to diverting the incident ray in various directions, away from the radar. Most studies have focused on researching surfaces with low reflection, such as FSS and metasurfaces.

A substantial amount of knowledge concerning passive techniques may be relied upon to regulate electromagnetic reflection and shielding. These passive methods often entail

manipulating or using radio absorbing materials (RAM). Frequency, incidence angle, and polarization of the impinging wave all influence the effectiveness of these techniques. The primary design goal is to reduce the amount of energy that is backscattered toward the radar. For monostatic radars, it has been discovered that this style of RCS control works well if the profile of a structure is created for an aeronautical vehicle, such as an airplane, a missile, or an unmanned aerial vehicle, in such way that the radar may only see a limited angular range [3].

Microwave absorbers consisting of periodic FSS have a variety of uses, including electromagnetic interference reduction, integrated circuit compatibility, backscatter reduction, stealth technology, light harvesting, and spacecraft, among others [4]–[7]. Numerous microwave absorbers have been constructed and their performance was using three major criteria: fractional bandwidth (FBW), figure of merit (FoM), and total thickness (TT) in wavelengths with regard to the lowest operating frequency (FL) [8]–[11].

Researchers have been concerned about FSS for decades, due to its potential applications in spatial microwave and optical filters [12], [13]. FSS are 2D or 3D periodic arrays of slots or patches imprinted on one or both sides of a single-layer or multilayer dielectric substrate. Because of the unique qualities of FSS, it has found several applications in RCS reduction, radar imaging, antennas, ideal lenses, and phase modulators [14], [15]. These structures are relied upon in various areas due to the increased operating frequencies of wireless systems. However, the main drawback of a bandpass FSS is its limited operational bandwidth. Because of the size constraints encountered in real-world applications, compact FSS must combine many unit cells in a single region to closely replicate ideal filtering behavior [16].

In this paper, the absorbing properties of FSS unit cell designs, as presented in [17], are developed and investigated. The approach adopted consists in adding a carbon paste layer to the copper layer printed on the substrate surface. Two FSS designs, in the form of double rings and double closed/split rings with added carbon paste, are proposed and investigated. The paper is organized as follows. Section 2 presents the basic design of the proposed unit cells, while Section 3 aims to add carbon paste to the double closed ring variety to obtain a larger bandwidth. Section 4 investigates another approach by adding carbon paste onto one region of the double closed/split inner ring to reduce the reflection coefficient. Section 5 investigates the same designs but after adding carbon paste onto two re-

gions to reduce the reflection coefficient. Section 6 studies the same approach by adding carbon paste onto three regions to achieve higher reduction in the reflection coefficient. The performance of all three proposed designs is compared in Section 7, while Section 8 presented the conclusions.

2. Proposed Unit Cells

The square form is employed in this particular design, since it provides comparable responses to the incident waves for vertical and horizontal polarizations and higher stability for the incidence angles [18]. Additionally, due to the multi-resonance characteristic of the double-ring design, this arrangement offers numerous advantageous qualities. The double-ring unit cell, as shown in Fig. 1a, and the double-closed-split ring, as shown in Fig. 1b, are constructed on an FR4 substrate with a 35 μm thick copper layer, a substrate layer thickness of $h_1 = 1.6$ mm, and relative permittivity of 4.3. The outer ring's side length L_1 is 15.6 mm, the breadth of each ring is 2 mm, and the unit cell dimensions are $L = 19 \times 19$ mm. The formula for the effective dielectric constant ϵ_e is [19]:

$$\epsilon_{eff} = \frac{\epsilon_r + 1}{2} + \frac{\epsilon_r - 1}{2} \left(1 + 12 \frac{h_1}{w} \right)^{-\frac{1}{2}}, \quad (1)$$

where h_1 is the substrate height, w is the ring width, and ϵ_r is the relative dielectric constant of the substrate. For the above parameters, the value of the effective dielectric is 3.16. The effective wavelength λ_e and the wavelength in air λ_o are determined by [17]:

$$\begin{aligned} \lambda_o &= \frac{c}{f}, \\ \lambda_e &= \frac{\lambda_o}{\sqrt{\epsilon_e}} = \frac{c}{f\sqrt{\epsilon_e}}, \end{aligned} \quad (2)$$

where f is the operating frequency, and c is the speed of light. The average circumferences of the outer ring CR_o and inner ring CR_i can be found from the geometry of Fig. 1 as:

$$\begin{aligned} CR_o &= 4(L_1 - w), \\ CR_i &= 4(L_2 - w). \end{aligned} \quad (3)$$

A closed conducting ring resonates when its average circumference equals the effective wavelength $CR_o = \lambda_{eo}$ [19]. Then, it can be shown that the resonance frequencies f_{ro} and f_{ri} for the outer and inner rings, respectively, as presented in Fig. 1a, are given by:

$$\begin{aligned} f_{ro} &= \frac{c}{CR_o\sqrt{\epsilon_e}}, \\ f_{ri} &= \frac{c}{CR_i\sqrt{\epsilon_e}}. \end{aligned} \quad (4)$$

The CST Microwave Studio software was used to model the above unit cells. The electric field of the incident wave is considered to be vertically oriented and to have linear polarization (along the v axis).

The geometry of the proposed unit cells is shown in Fig. 2, where the carbon layer is marked in black. The properties of the carbon paste are as follows: electric conductivity $\sigma = 1.2$ s/m, density $\rho = 1070$ kg/m³, and carbon thickness 35 μm. By including resistive material in the two types of the double ring

FSS cell, it was possible to track the results of the modification using the reflection coefficient S_{11} frequency response and evaluate the effect of the added paste layer.

3. Closed Rings Unit Cell with Paste

Figure 2 shows two approaches to adding the carbon paste: inter-ring, or inter-ring with a patch at the center of the unit cell. The variations of the reflection coefficient magnitude $|S_{11}|$ for these two cases are compared with the results obtained before the addition and are shown in Fig. 3. In the proposed unit cell of copper rings, the resonance frequency appears at 3.045 GHz, and with -10 dB bandwidth of 47 MHz. This case shows a higher second resonance frequency of 5.3 GHz, i.e. approximately twice that of the first result. This is due to the resonance of the inner ring whose circum-

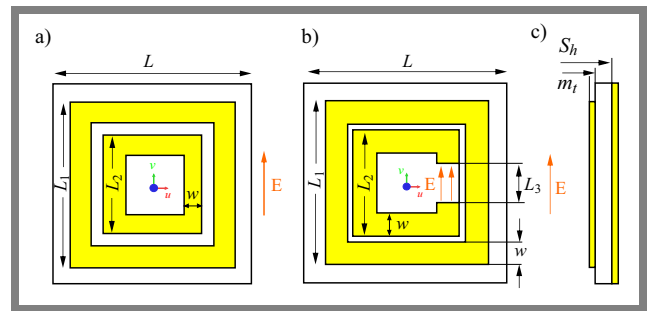


Fig. 1. Unit cell geometry: a) closed double-rings front view, b) closed/split double rings front view, and c) side view.

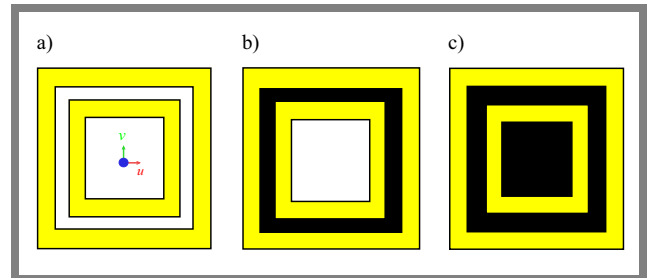


Fig. 2. Double-closed ring geometry of the unit cell: a) closed copper rings, b) carbon ring added, and c) carbon ring and patch at the center added.

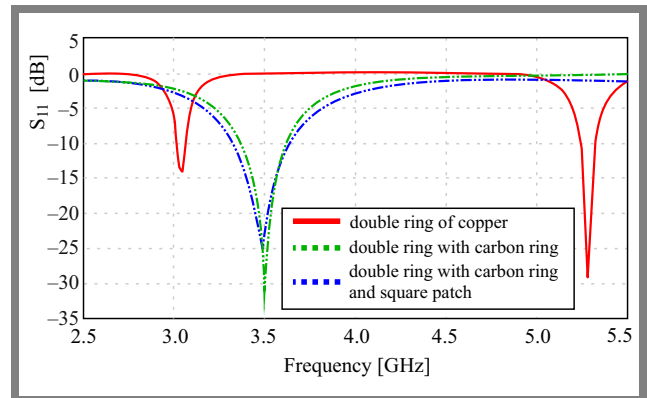


Fig. 3. Reflection coefficient-related outcomes of using copper rings, adding a carbon ring, and adding a carbon ring and a path at the center.

Tab. 1. Comparison of the reflection coefficient responses of the copper double closed rings unit cell before and after adding carbon paste.

Type of cell	Resonance frequency [GHz]	Bandwidth [GHz]	Minimum S_{11} [dB]
Copper rings only	3.045	0.0471	-14.1
Carbon ring	3.5	0.248	-30.4
Carbon (ring + square patch)	3.49	0.314	-24.8

Tab. 2. Comparison of the reflection coefficient responses for a double-split ring unit cell before and after adding carbon paste in one region.

Type of cell	Resonance frequency [GHz]	Bandwidth [GHz]	Minimum S_{11} [dB]
Copper rings only	3.48	0.172	-14.4
Square patch	3.53	0.051	-11.5
At the gap of inner ring	3.56	0.047	-11.3
Carbon ring	3.833	0.175	-22.9

ference is approximately half that of the outer ring. In this simulation, the outer and inner ring circumferences were 54.4 mm and 32.56 mm, respectively. In terms of the effective wavelength corresponding to the resonance frequency of the outer ring, the circumference is $0.982 \lambda_e$, and the relation corresponding to the inner ring is $1.024 \lambda_e$. Those figures are very close to the estimations presented in Eq. (4).

When a layer of carbon paste was placed between the two rings, the resonance frequency was shifted to 3.5 GHz, with a bandwidth of 248 MHz. The same resonance frequency was obtained when the central region of the unit cell was covered with the carbon paste. However, the bandwidth was increased to 314 MHz. The details of the three responses are illustrated in Tab. 1.

It is evident that a higher bandwidth was obtained for the scenario in which the paste was placed between the two rings. Adding a layer of paste at the center has increased the absorption by approximately 6 dB, and the bandwidth by approximately a 20%. The shift in the resonance frequency may be related to the effect of the resistive layer between the two copper rings. This added ring has resulted in an equivalent ring of a smaller circumference and, consequently, higher resonance frequency. The increase in the bandwidth can be understood as a result of adding resistive elements (carbon layers) that reduce the quality factor of the resonance structure, as the bandwidth is inversely proportional to the quality factor.

4. Open Inner Ring with Paste in One Region

The unit cell proposed in this section uses a double closed/split inner ring configuration and the same substrate as shown in Fig. 4. The idea behind this approach is to reduce the resonance frequency of the inner ring to a value near that of the outer ring, so that the two resonances merge and result in a larger bandwidth. Open or split rings resonate when their average length equals half the effective wavelength. Therefore, Eq. (4) is now developed for the split ring to be in the following form:

$$f_{ri} = \frac{c}{2CR_i\sqrt{\epsilon_e}}. \quad (5)$$

This gives the flexibility to choose the radius and gap of the inner split ring to tailor its frequency to a value that is close to that of the outer ring, without any overlap between the two rings.

Figure 4 shows the three scenarios involving adding carbon paste which were studied to find the best arrangement. As shown, the unit cell's dimensions are $L = 18 \times 18$ mm, the outer ring side length L_1 is 14.15 mm, the ring's width is $w = 0.1 \times L_1 = 1.56$ mm, and the inner ring size is $L_2 = 0.65 \times L_1 = 9.1975$ mm. The variations of the reflection coefficients with frequency changes, for the cases in which the carbon paste was inserted at one region, are compared with those before adding the carbon paste, as shown in Fig. 5. The response of the copper rings (red plot) shows two close dips corresponding to the inner and outer rings. The figure also illustrates that the insertion of the carbon paste either within the gap of the inner ring or at the center of the inner ring, to form an inter-ring layer, fails to significantly affect the minimum value of the reflection coefficient, but results in a bandwidth reduction. However, inserting the paste between the two rings reduces the minimum value of the reflection coefficient by approximately 8 dB, while preserving the bandwidth's value from before adding the paste.

The resonance frequency has increased by 0.3 GHz. A slight increase in the size of the rings can easily compensate for this frequency shift. As the effect of the carbon paste can be interpreted as a loss mechanism, placing the carbon paste in a region with an intense electric field will lead to a larger loss and, hence, a lower reflection coefficient.

5. Open Inner Ring with Paste in Two Regions

In the search for a lower reflection coefficient, it was decided to place the carbon paste on two regions of the unit cell. The geometries of the three placement scenarios are shown in Fig. 6. The obtained variations in the reflection coefficient with frequency changes are illustrated in Fig. 7.

It is evident that the addition of carbon paste between the two rings, as well as at the square patch at the center of the unit cell, has reduced the minimum value of the reflection coefficient by approximately 14 dB, simultaneously increasing bandwidth to

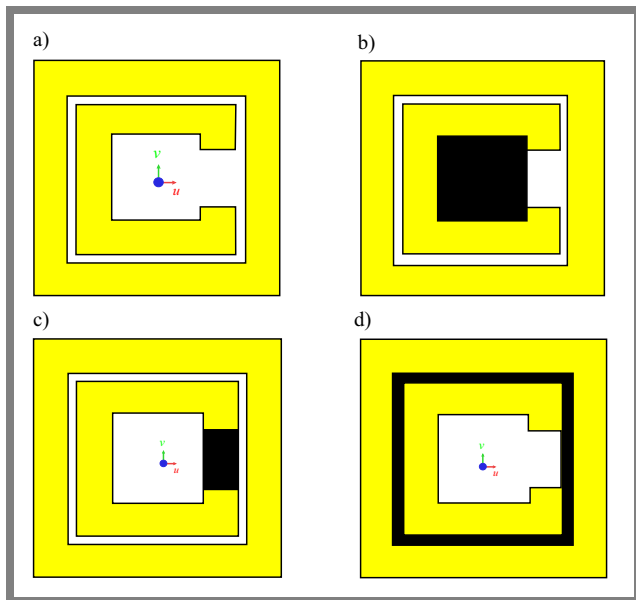


Fig. 4. Geometry of the double/split ring unit cell: a) before and b)–d) after adding carbon paste in one region.

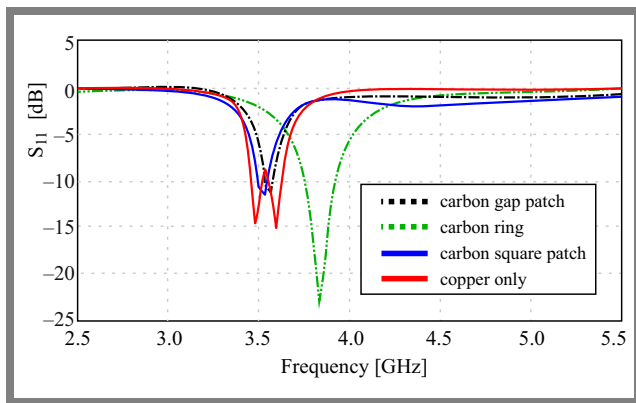


Fig. 5. Comparison of reflection coefficients for scenarios before and after adding carbon paste in one region.

approximately 282 MHz. This achievement is at the expense of increasing the resonance frequency by 8.6%. This shift in frequency may be compensated for by increasing the size of the rings. Table 3 shows a detailed comparison of the performance values for all four scenarios under consideration.

6. Open Inner Ring with Paste in Three Regions

For further improvement of the achieved results, the carbon paste was added to three regions to increase the area that absorbs the incident power. Thus, the surface of the FSS unit cell is now fully covered with either copper or carbon paste, as shown in Fig. 8. Figure 9 presents the reflection coefficient S_{11} obtained, compared with the case without any carbon paste. The addition of carbon paste results in a reduction in the minimum value of the reflection coefficient by approximately 4 dB, simultaneously increasing bandwidth to 326 MHz and changing resonance frequency to 3.88 GHz.

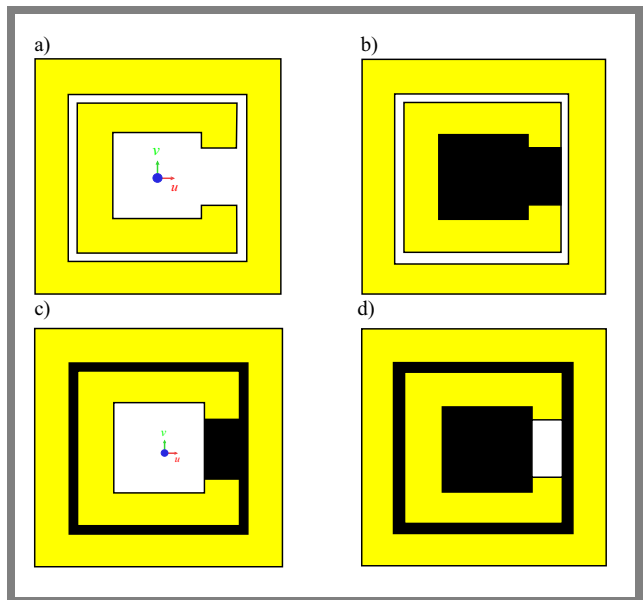


Fig. 6. Geometries of unit cells with carbon paste in two regions, compared with the copper ring scenario.

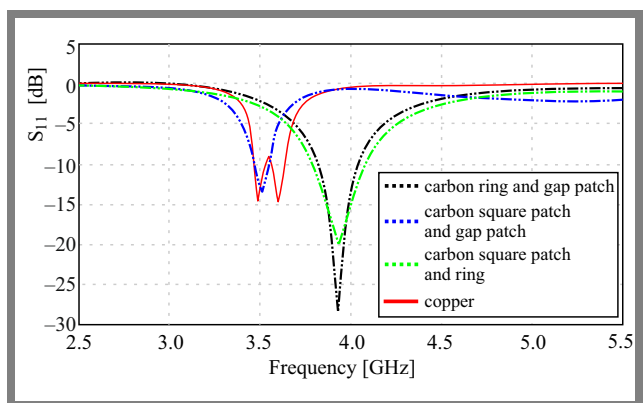


Fig. 7. Comparison of reflection coefficients for scenarios before and after adding carbon layer in two regions.

Tab. 3. Comparison of the performance of a double-split ring unit cell before and after adding carbon paste to two regions.

Region to which carbon was added	Resonance frequency [GHz]	Bandwidth [GHz]	Minimum S_{11} [dB]
Copper rings only	3.48	0.172	-14.4
Square patch and gap of the inner ring	3.5	0.082	-13.7
Ring and gap of the inner ring	3.8	0.224	-28
Ring and square patch	3.922	0.226	-20

7. Comparison of Results

Table 5 shows a detailed comparison of the results obtained in all three approaches to adding the carbon paste. For each

Tab. 4. Comparison of the performance of a double/split ring unit cell before and after adding carbon paste to three regions.

Type of cell	Resonance frequency [GHz]	Bandwidth [GHz]	Minimum S_{11} [dB]
Copper rings only	3.48	0.172	-14.4
Carbon in three regions	3.88	0.326	-18.44

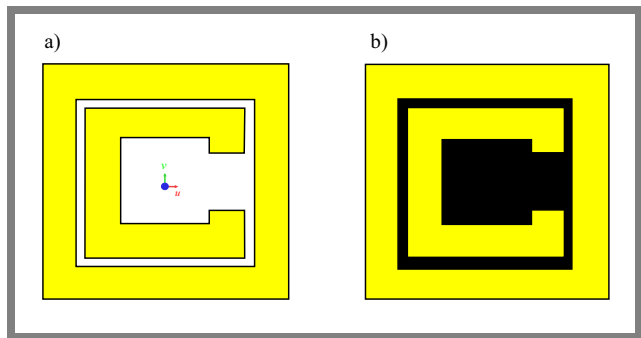
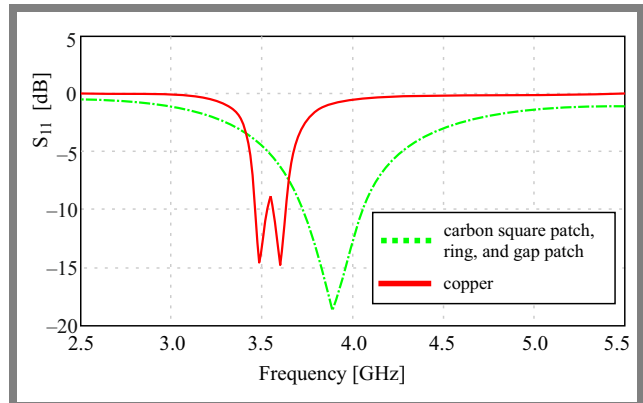
Tab. 5. Comparison of the performance of the three approaches to adding the carbon paste.

Type of cell	Resonance frequency [GHz]	Bandwidth [GHz]	Minimum S_{11} [dB]
Copper rings only	3.48	0.172	-14.4
One region carbon	3.833	0.175	-22.9
Two regions carbon	3.922	0.226	-28.74
Three regions carbon	3.88	0.326	-18.44

approach, the case of the best results was chosen for comparison purposes. The changes in the values of three features are evident. The first one is the increase in resonance frequency. This can be attributed to the fact that adding the carbon paste changes the estimated value of the effective dielectric constant ϵ_e . This latter parameter was estimated by the conventional empirical method using Eq. (1), which did not consider the existence of the carbon paste. Looking into Eq. (4), one can see that the resonance frequency increases when either the effective dielectric constant ϵ_e is decreased, or the effective circumference of the ring is reduced. Moreover, the carbon ring in between the two rings can be considered to form an equivalent smaller ring that results in a higher resonance frequency.

Bandwidth is the second parameter and it increased with the addition of carbon paste. The addition of a lossy layer will reduce the quality factor of the resonating structure, consequently increasing bandwidth. The third feature that needs to be noted is the reduction in the minimum value of the reflection coefficient. The last two findings (bandwidth increase and reflection coefficient reduction) are favorable features of adding the carbon layer.

Table 6 presents a comparison of the performance of the proposed unit cell (shown in Fig. 8) with other techniques that were described recently in the literature. The proposed unit cell showed a smaller bandwidth than the one in [21], while the other designs offer larger bandwidths. This can be attributed to the fact that dual-layer designs that incorporate an air gap can offer higher bandwidths, as one may notice in [21]–[25]. From the manufacturing point of view, adding

**Fig. 8.** Geometry of a double-split ring unit cell: a) before and b) after adding carbon paste in three regions.**Fig. 9.** Variation of the reflection coefficient of a double-ring unit cell (open inner ring) with carbon in three rings compared with the copper-only scenario.

a carbon paste layer is much easier than adding discrete resistances, as proposed in [20]–[23], where four resistors are needed per unit cell, or as in [24], where one lumped resistor and a via were used in each unit cell. In [23], four lumped resistors and a combination of three layers were used to achieve larger bandwidth. Moreover, the proposed design has a thickness of merely 1.6 mm, compared to the air-gapped design's overall thickness of 23.2 mm [21], and 17 mm [25]. Based on this comparison, the hardware designer is capable of implementing some compromise solutions to achieve the required goal.

8. Conclusions

This paper presented a method intended to enhance the performance of FSS unit cells in reducing radar cross-section. A carbon paste layer was added to a conventional design that used a copper layer on the top surface of the substrate. The simulations have demonstrated that the addition of a resistive material reduced the reflection coefficient by 4 to 8 dB, depending on the placement of the carbon paste. Moreover, an increase in bandwidth caused by the reduced quality factor was noticed as well. These findings make the proposed method advantageous compared with other approaches. From the manufacturing point of view, adding a carbon layer is simpler than inserting lumped resistors in the FSS unit cell.

Tab. 6. Comparison of the performance of the proposed unit cell and designs described in recent publications.

Reference	Type of cell	No. of layers	Size [mm]	Thickness [mm]	Frequency [GHz]	Bandwidth [GHz]
[20]	Four lumped resistances on copper ring	One	12.5×12.5	5	4–8	4–8.12
[21]	Four lumped resistances on copper ring	Two	20×20	23.2	0.91	0.15
[22]	Four lumped resistors on copper ring	Two	11.4×11.4	12, with foam	2.83–8.67	5.84
[23]	Four lumped resistors on meandered line	Two	10×10	12, with air	2.4–6.2	3.6
[24]	Resistor on rings and strips	Two	27×27	15.6, with air	5.43–5.87	0.44
[25]	Dipole and lumped resistors	Two	30×30	17, with air	2.8–5	2.2
This work (Fig. 8)	Three regions carbon	One	18×18	3.2	3.88	0.326

References


- [1] E.F. Knott, J.F. Schaeffer, and M.T. Tulley, *Radar cross section*, SciTech Publishing, 2nd ed., 2004 (<https://doi.org/10.1049/SBRA026E>).
- [2] R.L. Fante and M.T. McCormack, "Reflection Properties of the Salisbury Screen", *IEEE Transactions on Antennas and Propagation*, vol. 36, no. 10, pp. 1443–1454, 1988 (<https://doi.org/10.1109/8.8632>).
- [3] H. Singh and R.M. Jha, *Active Radar Cross Section Reduction: Theory and Applications*, Cambridge: Cambridge University Press, 2015 (<https://doi.org/10.1017/CB09781316136171>).
- [4] K.J. Vinoy and R.M. Jha, *Radar Absorbing Materials*, Kluwer Academic Publisher: Dordrecht, 209 p., 1996 (ISBN: 9781461380658).
- [5] F. Costa, S. Genovesi, and A. Monorchio, "A Chipless RFID Based on Multiresonant High-Impedance Surfaces", *IEEE Transactions on Microwaves Theory and Techniques*, vol. 61, no. 1, pp. 146–153, 2013 (<https://doi.org/10.1109/TMTT.2012.2227777>).
- [6] D. Kundu, A. Mohan, and A. Chakrabarty, "Single-layer Wideband Microwave Absorber Using Array of Crossed Dipoles", *IEEE Antennas and Wireless Propagation Letters*, vol. 15, pp. 1589–1592, 2016 (<https://doi.org/10.1109/LAWP.2016.2517663>).
- [7] J. Song *et al.*, "Broadband and Tunable Radar Absorber Based on Graphene Capacitor Integrated with Resistive Frequency-Selective Surface", *IEEE Transactions on Antennas and Propagation*, vol. 68, no. 3, pp. 2446–2450, 2020 (<https://doi.org/10.1109/TAP.2020.2943419>).
- [8] K.N. Rozanov, "Ultimate Thickness to Bandwidth Ratio of Radar Absorbers", *IEEE Transactions on Antennas and Propagation*, vol. 48, no. 8, pp. 1230–1234, 2000 (<https://doi.org/10.1109/8.884491>).
- [9] K.R. Jha, G. Mishra, and S.K. Sharma, "Design of a Compact Microwave Absorber Using Parameter Retrieval Method for Wireless Communication Applications", *IET Microwaves Antennas and Propagation*, vol. 12, no. 6, pp. 977–985, 2018 (<https://doi.org/10.1049/iet-map.2017.0785>).
- [10] J. Chen, Y. Shang, and C. Liao, "Double-layer Circuit Analog Absorbers Based on Resistor-Loaded Square-Loop Arrays", *IEEE Antennas and Wireless Propagation Letters*, vol. 17, no. 4, pp. 591–595, 2018 (<https://doi.org/10.1109/LAWP.2018.2805333>).
- [11] Y. Han, W. Che, C. Christopoulos, Y. Xiong, and Y. Chang, "A Fast and Efficient Design Method for Circuit Analog Absorbers Consisting of Resistive Square-Loop Arrays", *IEEE Transactions on Electromagnetic Compatibility*, vol. 58, no. 3, pp. 747–757, 2016 (<https://doi.org/10.1109/TEMC.2016.2524553>).
- [12] B.A. Munk, "Frequency Selective Surfaces: Theory and Design", Wiley, New York, 440 p., 2000 (<https://doi.org/10.1002/0471723770>).
- [13] N. Liu, X. Sheng, C. Zhang, and D. Guo, "Design of Frequency Selective Surface Structure with High Angular Stability for Radome Application", *IEEE Antennas and Wireless Propagation Letters*, vol. 17, no. 1, pp. 138–141, 2018 (<https://doi.org/10.1109/LAWP.2017.2778078>).
- [14] Y. Li *et al.*, "Compact Miniaturized-Element Frequency Selective Surface", *Electronics Letters*, vol. 51, no. 12, pp. 883–884, 2015 (<https://doi.org/10.1049/el.2015.0288>).
- [15] N. Choudhary, A. Sharma, and S. Yadav, "A Novel Band Stop Frequency Selective Surface for the Security of Quad Band Mobile Applications", *2017 IEEE Applied Electromagnetics Conference (AEMC)*, Aurangabad, India, 2017 (<https://doi.org/10.1109/AEMC.2017.8325687>).
- [16] N. Liu, X. Sheng, X. Gao, D. Guo, and R. Yang, "A Band-Pass Frequency Selective Surface with Wideband Rejection Characteristic", *2018 Asia-Pacific Microwave Conference (APMC)*, Kyoto, Japan, pp. 1286–1288, 2018 (<https://doi.org/10.23919/APMC.2018.8617503>).
- [17] M.B. Jasim and K.H. Sayidmarie, "Planar Absorbing FSS Unit Cells for Radar Cross-section Reduction", *IEEE 2022 International Conference on Innovation and Intelligence for Informatics, Computing, and Technologies (3ICT)*, Sakheer, Bahrain, pp. 476–480, 2022 (<https://doi.org/10.1109/3ICT56508.2022.9990893>).
- [18] Y. Li, M.E. Bialkowski, K.H. Sayidmarie, and N.V. Shuley, "81-Element Single-Layer Reflectarray with Double-Ring Phasing Elements for Wideband Applications", *2010 IEEE Antennas and Propagation Society International Symposium*, Toronto, Canada, 2010 (<https://doi.org/10.1109/APS.2010.5562103>).
- [19] K.H. Sayidmarie and T.A. Nagem, "Compact Dual-Band Dual-Omega Printed Monopole Antennas for WLAN Applications", *Progress in Electromagnetics Research B*, vol. 1, pp. 313–331, 2012 (<https://doi.org/10.13140/2.1.1195.5204>).
- [20] P. Munaga, S. Ghosh, S. Bhattacharyya, and K.V. Srivastava, "A Fractal-Based Compact Broadband Polarization Insensitive Metamaterial Absorber Using Lumped Resistors", *Microwave and Optical Technology Letters*, vol. 58, no. 2, pp. 343–347, 2016 (<https://doi.org/10.1002/mop.29571>).
- [21] W. Zuo, Y. Yang, X. He, D. Zhan, and Q. Zhang, "A Miniaturized Metamaterial Absorber for Ultrahigh-Frequency RFID System", *IEEE Antennas and Wireless Propagation Letters*, vol. 16, pp. 329–332, 2017 (<https://doi.org/10.1109/LAWP.2016.2574885>).

- [22] Q. Chen, M. Guo, Di Sang, and Y. Fu, "Polarization-Insensitive Frequency-Selective Rasorber Based on Square-Loop Element", *Progress in Electromagnetics Research M*, vol. 79, pp. 41–49, 2019 (<https://doi.org/10.2528/PIERM18110607>).
- [23] Z. Shen, N. Kou, S. Yu, Z. Ding, and Z. Zhang, "Miniaturized Frequency Selective Rasorber Based on Meander-Lines Loaded Lumped Resistors and a Coupled Resonator Spatial Filter", *Progress in Electromagnetics Research M*, vol. 90, pp. 147–155, 2020 (<https://doi.org/10.2528/PIERM20010503>).
- [24] M. Qu, S. Sun, L. Deng, and S. Li, "Design of a Frequency-Selective Rasorber Based on Notch Structure", *IEEE Access*, vol. 7, pp. 3704–3711, 2019 (<https://doi.org/10.1109/ACCESS.2018.2886421>).
- [25] Z. Wang *et al.*, "A High-Transmittance Frequency-Selective Rasorber Based on Dipole Arrays", *IEEE Access*, vol. 6, pp. 31367–31374, 2018 (<https://doi.org/10.1109/ACCESS.2018.2843795>).
-

Mustafa B. Jasim, M.Sc.

Department of Communication Engineering
College of Electronic Engineering
E-mail: mustafa.basim2021@stu.uoninevah.edu.iq
Ninevah University, Mosul, Iraq
<https://uoninevah.edu.iq>

Khalil H. Sayidmarie, Professor

Department of Communication Engineering
College of Electronics Engineering
 <https://orcid.org/0000-0001-6525-0949>
E-mail: kh.sayidmarie@uoninevah.edu.iq
Ninevah University, Mosul, Iraq
<https://uoninevah.edu.iq>